

1 **Molecular and functional characterization of a *Schistosoma bovis* annexin:**
2 **Fibrinolytic and anticoagulant activity.**

3

4 Eduardo de la Torre-Escudero¹, Raúl Manzano-Román¹, Mar Siles-Lucas¹, Ricardo
5 Pérez-Sánchez¹, J. Carlos Moyano², Inmaculada Barrera³, Ana Oleaga^{1*}.

6

7 ¹ Parasitology Laboratory, Instituto de Recursos Naturales y Agrobiología de Salamanca
8 (IRNASA, CSIC). Cordel de Merinas, 40-52, 37008 Salamanca, Spain.

9 ² Servicio de Análisis Clínicos. Complejo Hospitalario de Salamanca. Paseo de San
10 Vicente 58-182. 37007. Salamanca. Spain

11 ³ Departamento de Estadística. Facultad de Medicina. Universidad de Salamanca.
12 Alfonso X El Sabio s/n. 37007. Salamanca. Spain.

13

14 Corresponding author:

15 Dr. Ana Oleaga

16 Parasitology Laboratory.

17 IRNASA. CSIC.

18 Cordel de Merinas, 40-52

19 37008 Salamanca, Spain

20 Tel.: +34 923219606; fax: +34 923219609

21 *E-mail address:* ana.oleaga@irnasa.csic.es

22

23 **ABSTRACT**

24

25 Annexins belong to an evolutionarily conserved multigene family of proteins expressed
26 throughout the animal and plant kingdoms. Although they are soluble cytosolic proteins
27 that lack signal sequences, they have also been detected in extracellular fluids and have
28 been associated with cell surface membranes, where they could be involved in anti-
29 haemostatic and anti-inflammatory functions. Schistosome annexins have been
30 identified on the parasite's tegument surface and excretory/secretory products, but their
31 functions are still unknown. Here we report the cloning, sequencing, *in silico* analysis,
32 and functional characterization of a *Schistosoma bovis* annexin. The predicted protein
33 has typical annexin secondary and tertiary structures. Bioassays with the recombinant
34 protein revealed that the protein is biologically active *in vitro*, showing fibrinolytic and
35 anticoagulant properties. Finally, the expression of the native protein on the tegument
36 surface of *S. bovis* schistosomula and adult worms is demonstrated, revealing the
37 possibility of exposure to the host's immune system and thus offering a potential
38 vaccine target for the control of schistosomiasis in ruminants.

39

40 *Keywords:* Annexin; *Schistosoma bovis*; Plasminogen; Anticoagulant activity;
41 Tegument.

42

43

44

45 **1. Introduction**

46

47 Schistosomiasis is a parasitic disease affecting man and domestic and wild animals
48 that represents an important health and veterinary problem in many tropical and
49 subtropical areas of the world. *Schistosoma bovis* is a cosmopolitan trematode of
50 ruminants that can produce significant economic losses in endemic areas (Vercruysse
51 and Gabriel, 2005). In addition, studies on *S. bovis* are interesting from the perspectives
52 of both veterinary and human medicine because this species represents the genetic and
53 immunological analogue of the important human pathogen *S. haematobium* (Agnew et
54 al., 1989).

55 Like all schistosome species, *S. bovis* adult worms can survive in host blood vessels
56 for many years. In order to achieve such long survival times, parasites have molecules
57 that allow them to modulate immune and haemostatic host responses to their own
58 benefit (Pearce and MacDonald, 2002; Mountford, 2005; Secor, 2005; Ramajo-
59 Hernández et al., 2007; De la Torre et al., 2010). It is well known that a significant part
60 of schistosome evasion mechanisms are achieved by the parasite's inner and outer
61 tegument surface (Abath and Werkhauser, 1997). The tegument, besides the gut,
62 constitutes one of the most important host-parasite interchange surface, playing a role in
63 the parasite's nutrient uptake, excretion, osmoregulation, sensory reception, signal
64 transduction, and interaction with the host's immune and haemostatic systems (Jones et
65 al., 2004; van Hellemond et al., 2006; Ramajo-Hernández et al., 2007; De la Torre et al.,
66 2010). Thus, the tegument is a key parasite compartment to be mined for target
67 molecules in the development of new anti-schistosome vaccines and drugs. With this
68 aim, in the last years numerous investigations have focused on the identification and
69 characterization of molecules expressed by schistosomes in their tegument and surface

70 membranes (van Balkom et al., 2005; Braschi et al., 2006; Braschi and Wilson, 2006;
71 Pérez-Sánchez et al 2006, 2009; Skelly and Wilson, 2006; Mulvenna et al., 2010a;
72 Castro-Borges et al., 2011). As a result, annexins have been one of the molecules
73 frequently identified in the tegument of schistosomes.

74 Annexins are Ca^{2+} - and phospholipid-binding proteins that form an evolutionarily
75 conserved multigene family, its members being expressed throughout the animal and
76 plant kingdoms. Structurally, annexins are characterized by a highly α -helical and
77 tightly packed protein core domain, considered to represent a Ca^{2+} -regulated membrane-
78 binding module. Human annexins, designated A1 to A13 (except annexin A12, which
79 is unassigned), have been implicated in a broad range of biological processes such as
80 membrane trafficking and fusion, plasma membrane repair, anticoagulation, interaction
81 with cytoskeletal proteins and signal transduction (Gerke and Moss, 2002; Moss and
82 Morgan, 2004; Draeger et al., 2011). These soluble cytosolic proteins lack signal
83 sequences that direct them to the classical secretory pathway. Nevertheless, some
84 members of the family have consistently been identified in extracellular fluids. Binding
85 sites for extracellular annexins exist on the cell surface and several possible functions
86 for these proteins have been proposed. They include a role of annexin A5 as an
87 anticoagulant protein, a function of annexin A2 as an endothelial cell-surface receptor
88 for plasminogen and tissue-type plasminogen activator (t-PA), and the anti-
89 inflammatory activities of annexin A1 (Hajjar and Krishnan, 1999; Gerke and Moss,
90 2002; Cederholm et al., 2007).

91 Regarding schistosome annexins, several proteomic studies have identified them on
92 the tegument surface of *S. mansoni* (Braschi and Wilson, 2006; Castro-Borges et al.,
93 2011) and *S. japonicum* (Mulvenna et al., 2010a), as well as in the excretion-secretion

94 products of *S. bovis* (Pérez.Sánchez et al., 2006). Moreover, in a recent survey of draft
95 genomes for *S. mansoni* and *S. japonicum* (<http://www.schistodb.org>), Hoffmann et al.
96 (2010) identified 14 annexins from *S. mansoni*, 6 from *S. japonicum* and 1 from *S.*
97 *haematobium*. Of these, it is known that schistosome annexins 1, 3 and 5 are expressed
98 on the tegument of the adult parasite (Braschi and Wilson, 2006; Mulvenna et al.,
99 2010a; Catro-Borges et al., 2011). Hofmann et al. (2010) reported that annexins are
100 particularly noteworthy as surface-associated molecules of adult schistosomes and are
101 likely to be an abundant surface-related molecule of digeneans such as the human liver
102 fluke, *Opisthorchis viverrini*, which also expresses abundant surface annexins (Mulvenna
103 et al., 2010b). The physiological roles of these schistosome annexins are still unknown
104 although it has been speculated that they could play important roles in surface
105 maintenance, such as by ensuring the integrity of the membrane-membranocalyx
106 complex (Braschi and Wilson, 2006).

107 Unveiling the functions of schistosome annexins, and particularly whether they
108 exhibit extracellular activities such as those reported for the annexins of other organisms
109 (i.e., anticoagulant and fibrinolytic activities), is important as these extracellular
110 activities could be vital for schistosome development and survival. Accordingly, the
111 aims of the present work were to determine the physiological role of the annexin of *S.*
112 *bovis* adult worms regarding its potential fibrinolytic and anticoagulant activities and to
113 demonstrate its expression on the parasite surface at the host-parasite interface.

114

115 **2. Material and methods**

116

117 *2.1. Parasite material*

118 The life cycle of *S. bovis* was maintained at the laboratory by routine passage
119 through sheep, golden hamsters, and the intermediate snail host *Planorbarius*
120 *metidjensis*. Adult worms and lung schistosomula were recovered, respectively, from
121 infected sheep and hamsters as described in De la Torre-Escudero et al. (2010). Briefly,
122 lambs were infected with 2,000 cercariae and 4 months later they were sedated with 10
123 mg of ketamine per kg of live weight and sacrificed by bleeding through the jugular
124 vein.

125 Adult worms were recovered from mesenteric veins and washed in warm
126 phosphate buffered saline (PBS) pH 7.2 at 37°C. Worms were inspected
127 microscopically to verify their integrity and vitality, and immediately processed for
128 RNA extraction, the collection of a tegument extract (TG), and immunolocalization
129 studies. The tegument extract was obtained as described by Ramajo-Hernández et al.
130 (2007).

131 Lung schistosomula were obtained from hamsters, following the method of Gui
132 et al. (1995). The animals were infected through the skin with 1,000 cercariae by
133 bathing them individually (in a solution containing the cercariae) for 1 h. Six days after
134 infection, the hamsters were euthanatized and their lungs were removed, minced and
135 incubated in RPMI medium at 37°C for two hours on a rocker-shaker. The suspension
136 was sieved and live, intact schistosomula were collected with a 20 µl pipette. After three
137 washes in warm PBS, they were fixed in 4% formalin and stored at 4°C until use.

138 Animal experimentation was done according to the rules from the ethical and
139 animal welfare committee from the institution where the experiments were conducted
140 (IRNASA, CSIC), following the corresponding EU rules and regulations.

141

142 *2.2. RNA isolation, RT-PCR and cloning*

143 Total RNA from adult worms was isolated using the NucleoSpin RNA II kit
144 (Macherey-Nagel), following the manufacturer's instruction, and preserved at -80°C.

145 Reverse transcription was performed from total RNA using the first Strand
146 cDNA Synthesis kit (Roche). For PCR amplification of *S. bovis* annexin cDNA, primers
147 were designed from the *S. mansoni* and *S. japonicum* annexin sequences (GenBank
148 AF065599 and AY813612, respectively). The forward primer (ANXFW, 5'-
149 ATGGCYAAWRTTTCTGRATTTGG) was designed from the *S. mansoni* and *S.*
150 *japonicum* annexin consensus sequence. This primer was used in two amplifications
151 with two different reverse primers designed, respectively, from the *S. mansoni* and *S.*
152 *japonicum* annexin sequences (ANXRev1, 5'-TTATTGTTCTTCATTATATATTTTC;
153 ANXRev2, 5'- TTATTCACCTAGACCACATAATG).

154 PCR amplifications were performed in 35 cycles of 94°C for 40 s, 42°C for 40 s,
155 and 72°C for 1 min 30 s for the 5 first cycles, and 94°C for 40 s, 48°C for 40 s, and 72°C
156 for 1 min 30 s for the remaining 30 cycles. PCR products were electrophoresed in
157 agarose gel and the cDNA band corresponding to the ANXFW/ANXRev2 amplification
158 was purified from the gel using the StrataPrep DNA Gel Extraction kit (Stratagene).
159 This PCR product was cloned into the pSC-A vector using the StrataClone PCR
160 Cloning kit (Stratagene), following the manufacturer's instruction, and sequenced on
161 both strands. At least three different clones of the insert were sequenced to check for
162 errors caused by PCR amplification.

163

164 2.3. Bioinformatic analysis

165 The deduced amino-acid sequence of *S. bovis* annexin (SbANX) was analyzed
166 as follows: BLAST searching of the most similar sequences were conducted in the
167 Swissprot/Uniprot and SchistoDB databases (<http://www.uniprot.org/> and

168 <http://www.genedb.org/Homepage/Smansoni>); analysis of conserved domains was
169 performed using SMART at <http://smart.embl-heidelberg.de>; theoretical isoelectric
170 point (pI) and molecular weight (MW) calculations at
171 http://www.expasy.org/tools/pi_tool.html; prediction of transmembrane helices using
172 the TMHMM Server v. 2.0 at <http://www.cbs.dtu.dk/services/TMHMM-2.0>; prediction
173 of signal peptides with SignalP 3.0 (Bendtsen et al., 2004) at
174 <http://www.cbs.dtu.dk/services/SignalP>, and search for glycosyl-phosphatidyl anchors
175 in the sequence with the big-PI Predictor (Eisenhaber et al., 2000) at
176 http://mendel.imp.ac.at/sat/gpi/gpi_server.html.

177 The amino acid sequence and secondary structure of the SbANX were compared
178 to those of four parasite and human annexins known to possess fibrinolytic or
179 anticoagulant activities, namely, the *Taenia solium* B1 and B2 (ANX B1, ANX B2) and
180 the human A2 and A5 (ANX A2, ANX A5). Multiple sequence alignment of all these
181 five annexins was done with ClustalW 2.1 at
182 <http://www.ebi.ac.uk/Tools/msa/clustalw2/>. For the prediction of the secondary
183 structures and three-dimensional modelling, the amino acid sequences were submitted
184 to the Swiss-Model server (Arnold et al., 2006) at <http://swissmodel.expasy.org/>. The 3-
185 D models were visualized using the Pymol package (DeLano, 2002).

186

187 2.4. Expression and purification of recombinant annexin and polyclonal antibody 188 production

189 The full-length cDNA sequence of SbANX was subcloned into the expression
190 vector pQE-30 (Qiagen) and expressed in *Escherichia coli* M15 cells (Qiagen). For this,
191 two new primers were designed from the *S. bovis* complete annexin sequence that
192 contained KpnI adapters to assist in the subcloning (sense primer; 5'-

193 GGGGTACCATGGCTAATGTTTCTGAATTTGG; antisense primer, 5'-
194 GGGGTACCTTATTCACCAAGTAGAACAC) (underlined letters represent the
195 restriction enzyme sites). The complete cDNA coding sequence of *S. bovis* annexin was
196 amplified from the SbANX-pSC-A construction. PCR amplification was accomplished
197 under the following conditions: 35 cycles of 94°C for 15 s, 64°C for 30 s and, 72°C for
198 40 s. The amplified product was purified using the DNA Gel extraction kit (Stratagene)
199 and digested with KpnI restriction endonuclease (Roche). After digestion, the PCR
200 product was purified again from agarose gel and ligated to the KpnI predigested pQE-30
201 vector. This construct was used to transform *E. coli* M15 cells. Single recombinant
202 clones were selected and plasmid DNA extracted and sequenced to confirm the presence
203 and the correct orientation of the SbANX cDNA insert.

204 Expression was then induced in correctly transformed *E. coli* M15 cells by
205 adding isopropyl β -d-thiogalactopyranoside (IPTG) at a final concentration of 1 mM at
206 37°C for 3h. The induced cells were harvested and lysed by sonication in a lysis buffer
207 containing 50 mM NaH₂PO₄, 300 mM NaCl, 10 mM imidazole, pH 7.9. After a 15 min
208 centrifugation step at 40,000g, the lysate pellet was solubilised in binding buffer
209 containing 100 mM NaH₂PO₄, 10 mM Tris-Cl, and 8M urea, and re-centrifuged as
210 above. The new supernatant was passed through His-Bind resin (Qiagen) according to
211 the manufacturer's instructions. Before elution of the recombinant, urea was eliminated
212 by washing the column with wash buffer (100 mM NaH₂PO₄, 10 mM Tris-Cl, pH 6.3)
213 containing decreasing concentrations of urea (6M, 4M, 2M). Then, the recombinant
214 protein was eluted with elution buffer (250 mM imidazole, 0.5 M NaCl, 50 mM
215 NaH₂PO₄, pH 7.9). The eluted rSbANX was dialysed against PBS for 24 h at 4°C and
216 stored at -80°C until use. The concentration of the recombinant protein was measured
217 using the DC Protein assay kit (Bio-Rad) and its purity was checked by SDS-PAGE.

218 Once the recombinant protein had been obtained, and in order to have a specific
219 probe for immunofluorescence studies, a polyclonal rabbit serum against *S. bovis*
220 annexin (rSbANX) was obtained. To accomplish this, two rabbits (New Zealand) were
221 immunized subcutaneously with three doses of 100 µg of rSbANX, together with
222 Freund's adjuvants. The first dose was administered with the complete adjuvant, the
223 second one with incomplete adjuvant and the third one only in PBS. The rabbits were
224 bled at 15 days after the third dose and the antibody titre was determined by ELISA,
225 using a standard protocol (Oleaga-Pérez et al., 1994).

226 The reactivity and specificity of the polyclonal serum was tested by Western
227 blotting against rSbANX and a tegument extract (TG) from adult worms following the
228 protocol described by De la Torre-Escudero et al (2010). In this case the anti-rSbANX
229 rabbit serum was used at a dilution of 1/1,600 and the peroxidase-conjugated anti-rabbit
230 antibody (Sigma) was diluted at 1/1,000.

231

232 *2.5. Bioassays with rSbANX*

233

234 *2.5.1. Plasminogen binding assays.*

235 The binding of rSbANX to plasminogen was assessed by ELISA in a similar
236 way to that described for the *S. bovis* enolase (De la Torre-Escudero et al., 2010).
237 Briefly, plate wells were coated with 0.5 µg of rSbANX and non-specific binding sites
238 were blocked with 1% BSA in PBS (PBS-BSA). After washing, the different wells were
239 incubated with increasing amounts (from 0 to 3 µg) of human plasminogen (Acris
240 Antibodies) diluted in PBS-BSA. After a new wash, the wells were incubated with
241 peroxidase-conjugated goat anti-human plasminogen IgG (Cedarlane Laboratories)
242 diluted 1/2,000 in PBS-BSA and finally ortho-phenylenediamine (OPD) was used as a

243 chromogenic substrate for peroxidase. The plate included negative control wells, coated
244 only with BSA, and positive control wells, coated with 1 µg of TG extract.

245 To assess whether plasminogen binding to rSbANX occurs through lysine
246 residues, a similar assay was performed in which the plate wells were coated with 0.5
247 µg of rSbANX and incubated with 0.5 µg of plasminogen and increasing concentrations
248 (from 0 to 60 mM) of ε-aminocaproic acid (εACA, Sigma). εACA is a lysine analogue
249 that competitively inhibits plasminogen from binding to its receptor. Then, bound
250 plasminogen was developed by incubating with peroxidase-conjugated goat anti-human
251 plasminogen IgG and OPD. Similarly, BSA-coated wells were used as negative
252 controls.

253

254 2.5.2. Plasminogen activation assays.

255 The effect of rSbANX on plasminogen activation and plasmin generation was
256 evaluated by measuring the amidolytic activity of newly generated plasmin on the
257 chromogenic substrate D-Valyl-L-leucyl-L-lysine 4-nitroanilide dihydrochloride
258 (Sigma). This assay was performed on ELISA plates according to the protocol described
259 previously (Mundodi et al., 2008).

260 In each plate well, 2 µg of plasminogen, 3 µg of chromogenic substrate, 1 µg of
261 rSbANX, and 15 ng of tissue-type plasminogen activator (t-PA) (Acris antibodies) were
262 mixed in a total volume of 150 µl of PBS and incubated at room temperature. In a
263 parallel assay, plasmin generation was measured in the absence of t-PA, in the absence
264 of rSbANX, and substituting annexin by BSA or by the buffer in which the rSbANX
265 had been dissolved. Plasmin generation was monitored by quantifying the hydrolysis of
266 the substrate through absorbance measurements at 405 nm every 30 min over two hours

267 as from the time the reaction began. Each reaction was analysed in quadruplicate and
268 the whole assay was repeated three times.

269

270 2.5.3. Prothrombin time and activated partial thromboplastin time of rSbANX.

271 The anticoagulant activity of rSbANX was analysed in two coagulation tests for
272 general screening such as the prothrombin time (PT) and the activated partial
273 thromboplastin time (aPTT) tests. The PT and aPTT tests respectively detect
274 disturbances in the extrinsic and intrinsic coagulation pathways. These tests measure the
275 time elapsed between the addition of the corresponding coagulation initiation reagent
276 (STA neoplastin plus or STA aPTT; Roche Diagnostics) to the plasma sample and clot
277 formation. The PT results can also be expressed as a percentage of the normal activity.

278 To carry out these tests, plasma samples were obtained from lamb blood
279 extracted in polypropylene tubes containing sodium citrate. The samples analysed
280 consisted of 500 µl of plasma with increasing amounts of rSbANX (from 0 to 80
281 µg/ml). Two series of control samples were included in the analysis: one series
282 contained BSA instead of rSbANX, and the other one contained no protein but
283 equivalent volumes of the buffer in which the rSbANX had been dissolved.

284 Each sample was analysed in duplicate and the assays were repeated twice.
285 Samples were analysed with the STA-R Evolution® analyser (Diagnóstica Stago, Inc.).

286

287 *2.6. Immunolocalization of annexin in adult worms and lung-stage schistosomula*

288 Tissue expression of annexin was determined in adult worms and schistosomula
289 by indirect immunofluorescence and later analysis by confocal microscopy. The study
290 was carried out on sections of adult worms, on whole adult worms, and on 6-day old

291 lung schistosomula. The worms were fixed in formaldehyde buffered at 4% for either 5
292 h (schistosomula) or 24 h (adults).

293 For assays on adult sections, the worms were dehydrated and embedded in
294 paraffin following standard protocols. Microtome-cut 5- μ m sections were placed on
295 microscope slides, deparaffinised in xylene, and rehydrated. The sections were then
296 blocked with 1% BSA in PBS containing 0.05% Tween 20 (PBST) for 1 h at 37°C,
297 after which they were incubated with the anti-rSbANX rabbit serum diluted 1/50 in
298 blocking buffer for 1 h at 37°C. Samples were washed three times with PBST and
299 incubated at 4°C overnight with an anti-rabbit IgG antibody conjugated to Alexa Fluor
300 594 (Invitrogen) diluted 1/400 in blocking buffer containing phalloidin-Alexa Fluor 488
301 (Invitrogen) diluted 1/200, which binds to actin microfilaments. The samples were then
302 washed four times and mounted in antifade reagent (Prolong Gold, Invitrogen). All
303 incubations were performed in a humid chamber.

304 A similar protocol was followed for whole-mount assays. The reactions were
305 performed in 1.5-ml test tubes containing 100 schistosomula or 5 adult pairs each. Fixed
306 parasites were blocked for 2 h at room temperature, incubated with the anti- rSbANX
307 serum overnight at 4°C, and then with the above-mentioned Alexa Fluor reagents, both
308 at a 1/300 dilution, for 4 h at room temperature. Whole parasites were washed five times
309 and then mounted in antifade reagent (schistosomula) or in PBS (adult worms). In each
310 assay, serum from a non-immunized rabbit was used as a negative control. Samples
311 were analysed with a Leica TCS-NT confocal microscope.

312

313 2.7. Statistics

314 The results of the PT and aPTT coagulation tests were first analysed with the
315 one-way ANOVA test, and when significant differences were found a *post hoc* analysis

316 with the HDS Turkey test was conducted to determine the causes of the significance. A
317 similar procedure was applied to check whether there were any significant differences
318 as a function of the amount of rSbANX added to the plasma samples and, if so, to
319 establish which rSbANX concentration provided significantly different results.

320

321 **3. Results**

322

323 *3.1. Cloning and in silico characterization*

324 The ANXFw/ANXRev2 primer pair amplified a 1080 bp cDNA fragment
325 compatible with the expected size for a schistosome annexin and an open reading frame
326 coding for a protein of 359 amino acids, with a predicted MW and pI of 40,663 Da and
327 5.85, respectively (GenBank accession number EU595758).

328 BLAST searching of the SWISS-Prot database with the deduced amino acid
329 sequence of SbANX retrieved numerous annexins from different species. *S. bovis*
330 annexin showed the highest identity percentages with the *S. mansoni* (Q9XY89) and *S.*
331 *japonicum* (AAW25344) annexins (91% and 86%, respectively). Similarly, BLAST
332 searching of the SchistoDB database retrieved several annexin sequences including the
333 14 annexins sequences of *S. mansoni* reported by Hofmann et al. (2010). Among them,
334 the sequence showing the highest identity (91%) was Sm_074150, which corresponds to
335 sequence Q9XY89 from the SWISS-Prot database; the remaining 13 sequences
336 retrieved showed lower identities (from 37% to 23%).

337 Regarding non-schistosome helminths, SbANX showed the greatest identity to
338 *Taenia solium* ANX B1 and B2 (42% and 36%, respectively). Finally, SbANX showed
339 between 37% and 23% sequence identity to human annexins A1-A13, in particular 37%
340 to ANX A5 and 32% to ANX A2.

341 Fig. 1A shows the alignment of SbANX with *T. solium* B1 and B2 and human
342 A2 y A5 annexins. The SbANX contained a 309-amino acid core domain and a 50-
343 amino acid tail at its N-terminus. The core domain contained the four typical annexin
344 repeats and each repeat harboured type II and III Ca²⁺-binding sites (Fig. 1A, yellow-
345 shaded and underlined residues, respectively). Type II calcium-binding sites were
346 characterized by the M-K/R-G/R-X-G-T-(38 residues)-D/E sequence motif, and type III
347 sites by the G-X-G-T-D/E sequence motif. In SbANX, each annexin repeat contained
348 between 52 and 60 amino acid residues, mapping in the following sequence segments:
349 51-103, 123-183 229-281 and 304-356 amino acid. The *E*-values for the four annexin
350 repeats ranged from 2.70e⁻²⁰ to 113e⁻⁰⁴. (Fig. 1A).

351 The SbANX contains the KGLGT sequence motif within repeat II of the core
352 domain as *T. solium* ANX B1 and human A2 annexins. In human A2 annexin, this motif
353 and the aspartic acid located at position 162 (D¹⁶²) appear to be required for the
354 interaction of annexin with cell surface phospholipids (Fig. 1A) (Hajjar and Krishnan,
355 1999).

356 The SbANX also had the ¹⁰⁰LCQL^{103/114}SL¹¹⁵ sequence motif, which showed
357 50% identity with the ⁸LCKLSL¹³ sequence motif of human ANX A2. This motif is
358 responsible for the interaction between human ANX A2 and t-PA (Hajjar et al., 1998).
359 A similar motif (³⁸LCK^{40/69}SL⁷⁰) is also displayed by the *T. solium* ANX B2. In Fig. 1B,
360 the above-mentioned motif is highlighted only in the 3D model of SbANX, but not in
361 that of ANX A2 because this molecule was modelled from the 32st amino acid onwards
362 not including the N-terminus fragment in which the motif is located.

363 SbANX and *T. solium* ANX B1 and B2 have an insert fragment in the linker
364 region between repeats II and III, which is absent from human annexins (Figs. 1A and
365 1B).

366 *In silico* secondary structure prediction revealed that SbANX was mainly made
367 up of α -helices although four beta sheets are also included. The model does not predict
368 secretory signal, transmembrane helices or glycosyl-phosphatidyl inositol anchors. The
369 secondary and tertiary structures of these annexins are highly conserved even though
370 their amino acid sequence identity only ranges between 32% and 42% (Fig. 1). The
371 alignment in Fig. 1A shows that the four typical annexin repeats and the predicted α -
372 helices match in the five sequences. In Fig. 1B it can be observed that the four repeats
373 are packed in a structure that resembles a flattened disc, with a slightly convex surface
374 on which the Ca^{2+} -binding loops are located, together with a concave surface where the
375 amino and carboxyl termini come into close opposition.

376

377 *3.2. Expression and purification of recombinant S. bovis annexin*

378 The full length SbANX cDNA was sub-cloned into the expression vector pQE-
379 30 and transformed into M15 *E. coli* host cells. The his-tagged recombinant protein
380 (rSbANX) was expressed abundantly, although it was 100% insoluble. After
381 solubilisation and purification under denaturing conditions, 5.7 mg of protein per litre of
382 cell culture was obtained. The purified rSbANX migrated as a single band of 39 kDa by
383 SDS-PAGE.

384

385 *3.3. Plasminogen binding and activation assays*

386 The plasminogen-binding assays showed that plasminogen bound to rSbANX
387 and that the amount of plasminogen bound increased with the rising amount of
388 plasminogen added to the reaction medium. Likewise, in the plate wells in which
389 tegument extract (TG) was included as a positive control in the assay the binding of the
390 plasminogen to such proteins was observed. In the negative control wells, coated only

391 with BSA, unspecific binding of plasminogen did not occur (Fig. 2A). Competition
392 experiments with ϵ ACA revealed that plasminogen binding occurred through lysine
393 residues, and that 10 mM of ϵ ACA completely inhibited the binding of plasminogen to
394 rSbANX (Fig. 2B).

395 Fig. 3 shows the results of the assays on plasminogen activation, in which it may
396 be seen that rSbANX enhanced plasminogen activation in the presence of t-PA. It can
397 also be observed that rSbANX was unable to activate plasminogen and generate
398 plasmin in the absence of t-PA. In the controls, in which rSbANX was replaced by BSA
399 or by buffer, no reactivity was observed (not shown).

400

401 *3.4. Anticoagulant activity*

402 To investigate the anticoagulant effect of rSbANX, we evaluated the inhibition
403 of blood clotting in PT and aPTT assays (Figs. 4A and 4B).

404 Both assays revealed significant differences ($p < 0.01$) between the samples with
405 rSbANX and the controls with BSA or buffer. Additionally, there were no significant
406 differences between either type of control sample (those containing BSA or buffer).

407 The coagulant activity in the PT assay was lower in the plasma samples with
408 rSbANX than in the controls and clearly decreased as the concentration of annexin
409 increased. This difference was statistically significant ($p < 0.01$) in the samples
410 containing a concentration of 80 μ g/ml of annexin with respect to the controls without
411 it. Likewise, coagulation time increased in parallel with the concentration of rSbANX.
412 This increase in coagulation time was significant at rSbANX concentrations equal to or
413 higher than 60 μ g/ml (Fig. 4A).

414 The anticoagulant effect of rSbANX was considerably stronger in the aPTT
415 assay. In this assay, the coagulation time was significantly longer ($p < 0.01$) as from an
416 rSbANX concentration of 10 µg/ml in plasma (Fig. 4B).

417

418 *3.5. Reactivity and specificity of the anti-rSbANX rabbit hyperimmune sera*

419 The reactivity of the anti-rSbANX hyperimmune serum was tested in ELISA
420 against the recombinant protein prior to its use in the immunolocalization assays. The
421 antibody titre was 1/1,600. The specificity of the serum was assessed by Western
422 blotting against the rSbANX and the native TG extracts from *S. bovis* adult worms. As
423 shown in Fig. 5, the anti-rSbANX serum reacted strongly with the recombinant protein
424 and specifically recognized the native annexin in the TG extract. The negative serum
425 showed no reactivity with any of the proteins tested.

426

427 *3.6. Immunolocalization of S. bovis annexin*

428 Annexin localization in the parasite was analyzed in paraffin sections from adult
429 worms, as well as in intact adult worms and 6-day-old lung schistosomula.

430 The schistosomula incubated with the negative rabbit serum plus phalloidin (an
431 actin ligand) only resulted in green fluorescence, indicating a lack of non-specific
432 reactivity. The schistosomula incubated with the specific anti-rSbANX serum plus
433 phalloidin showed actin reactivity in green, as well as the specific annexin reactivity
434 (red) distributed on the tegument surface (Fig. 6). This figure shows the images
435 obtained at each of the laser wavelengths -594 (red) and 488 (green)- since the merged
436 image was difficult to interpret due to the co-localization of the specific reaction and the
437 actin fluorescence.

438 Paraffin-embedded sections from adult worms incubated with the negative
439 serum plus phalloidin resulted in green fluorescence on the outermost part of the
440 tegument. Sections of male and female worms incubated with the specific anti-rSbANX
441 serum plus phalloidin showed besides the actin reactivity in green the specific annexin
442 reactivity, in red, abundantly distributed in internal tissues and also in the tegument
443 surface. In male tegument, the red signal appears as discontinuous patches (arrows) and
444 in female tegument, apparently, as a more continuous signal (Fig. 7A).

445 Whole adult worms incubated with negative serum only showed the green
446 fluorescence from actin. By contrast, adult worms incubated with the anti-rSbANX
447 serum showed a red fluorescence pattern on the outermost part of the tegument. In
448 males this pattern consisted of low abundant scattered tiny patches, and in females these
449 patches were similarly distributed but more abundant (Fig. 7B).

450

451 **4. Discussion**

452

453 It is well known that schistosomes have adapted to the intravascular habitat of
454 their hosts by developing mechanisms to modulate the haemostatic response. However,
455 despite the relevance of the molecules involved in the biology of the parasite and their
456 potential interest as vaccine antigens, these haemostatic molecules have aroused little
457 attention.

458 This prompted us to undertake studies of the interaction of *S. bovis* with the
459 host's haemostatic system. In previous work, we observed that adult worms activate the
460 fibrinolytic system, presumably as a strategy to prevent the formation of clots around
461 them, and that they did this through protein receptors for plasminogen expressed on the
462 surface of their tegument, one of which has been determined to be enolase (Ramajo-

463 Hernandez et al., 2007; De la Torre-Escudero et al., 2010). Here we wished to
464 determine whether the annexin of *S. bovis* possesses any anti-haemostatic activity. In
465 this sense, for some time it has been known that other annexins, such as the human A2
466 and A5 and the B1 and B2 annexins of *T. solium* show anticoagulant and fibrinolytic
467 activities (Hajjar et al., 1999; Gerke and Moss, 2002; Wang et al., 2006; Winter et al.,
468 2006). So we cloned and sequenced the *S. bovis* annexin cDNA and obtained a peptide
469 sequence of 359 amino acids that displayed structural characteristics typical of the
470 annexin family. That is, a core domain containing four typical annexin repeats
471 characterized by alpha-helices and a variable N-terminal region (Gerke and Moss,
472 2002). In this way, we confirmed the fact, already observed in vertebrate annexins, that
473 the secondary and tertiary structures of annexins are highly conserved despite not
474 showing high amino acid sequence identity among themselves (Moss and Morgan,
475 2004).

476 One particularity of the SbANX sequence, that human annexins do not have, is
477 the long linker region between repeats II and III. This characteristic is also seen in other
478 schistosome annexins and in those of *T. solium* (Wang et al., 2006; Hofmann et al.,
479 2010; Tararam et al., 2010). As reported by Hofmann et al. (2010), these unique
480 structural features combined with the immunogenic properties of several parasite
481 annexins and unique epitopes not present in mammalian annexins may provide an
482 opportunity to pursue these antigens as vaccine targets while preventing cross-reactivity
483 with host annexins.

484 Sequence analysis also revealed that SbANX lacks motifs for its transport or
485 expression on the cell surface (signal peptide, transmembrane motif or GPI anchors),
486 even though it is present on the surface of schistosomula and adult worms. This is not
487 an isolated phenomenon since the same occurs with other annexins, and in particular

488 with human A2 annexin, which is constitutively expressed on the endothelial cell
489 surface and the mechanism of its export from the cell is unknown. It has been described
490 that human annexin A2 interacts with cell surface phospholipids via a calcium-
491 dependent binding site that includes ¹¹⁹KGLGT¹²³ residues and the coordinating D¹⁶² of
492 core repeat 2 (Hajjar and Krishnan, 1999). In the *S. bovis* annexin we found the same
493 motif in residues 120-124 (¹²⁰KGLGT¹²⁴) as well as a D¹⁶⁷. It is therefore possible that
494 this motif could be responsible for the interaction between the *S. bovis* annexin and the
495 phospholipids of the plasma membrane at the surface of the tegument of the worms,
496 although confirmation of this point requires additional studies.

497 The plasminogen binding and activating assays indicated that the *S. bovis*
498 annexin, like the human A2 annexin (Hajjar et al., 1998), had fibrinolytic activity. It
499 was observed that rSbANX binds plasminogen through lysine residues and that it
500 enhanced t-PA mediated plasminogen activation. This is the first time that
501 profibrinolytic activity has been demonstrated in an annexin of parasite origin, and
502 particularly in a schistosome species.

503 Human A2 annexin interacts with t-PA through the ⁸LCKLSL¹³ motif present at
504 the N-terminal end (Hajjar et al., 1998). In the rSbANX sequence, a similar motif has
505 been identified with an identity of 50% (¹⁰⁰LCQL^{103/114}SL¹¹⁵). However, despite this
506 similarity it does not seem likely that this motif would be responsible for the interaction
507 with t-PA since, as seen from the three-dimensional model of rSbANX, it is localized in
508 a zone of the molecule that is not very accessible (Fig. 1B).

509 The A5 extracellular annexin shows anticoagulant properties that depend on its
510 Ca²⁺-regulated binding to anionic phospholipids; those exposed on the surface of
511 activated platelets or endothelial cells. In the presence of Ca²⁺ annexin competitively
512 binds to phospholipids with very high affinity and disturbs the form of some activated

513 coagulation complexes (Gerke and Moss, 2002). Regarding this type of activity, in
514 known parasite annexins anticoagulant properties have only been demonstrated for the
515 annexins B1 and B2 of *T. solium* (Wang et al., 2006). In *S. bovis*, the results of the PT
516 and aPTT assays clearly demonstrate that rSbANX inhibits the extrinsic coagulation
517 pathway and, more strongly, the intrinsic pathway. Inhibition of the extrinsic
518 coagulation pathway was achieved with high concentrations of rSbANX (60-80 µg/ml),
519 which were higher than those of *T. solium* annexin B2 producing the same effect (40
520 µg/ml); by contrast, inhibition of the intrinsic pathway was achieved with quite lower
521 rSbANX concentrations (10 µg/ml) as compared to *T. solium* annexin B1 (60 µg/ml)
522 (Wang et al., 2006).

523 Thus, this would be the first demonstration of anticoagulant activity by an
524 annexin from a Schistosoma species. Additionally, bearing in mind the different
525 functions of vertebrate annexins, it cannot be ruled out that *S. bovis* annexin could have
526 additional activities, in particular some type of immunomodulatory activity, as has been
527 demonstrated for the B1 *T. solium* annexin (Gao et al., 2007; Yan et al., 2008).

528 It is evident that for these anticoagulant and fibrinolytic activities of SbANX to
529 have relevant physiological roles, the SbANX should be exposed on the surface of the
530 worm into contact with the host blood. As reported in different studies addressing the
531 tegument of schistosomes, annexin has been identified on the tegument surface of adult
532 worms and schistosomula of *S. mansoni* and *S. japonicum* (Braschi and Wilson, 2006;
533 Tararam et al., 2010; Castro-Borges et al., 2011). The SbANX immunolocalization
534 studies performed in adults and schistosomula of *S. bovis* indicate that both
535 developmental stages express this protein on the surface of their tegument. The
536 schistosomula of *S. bovis* shows an annexin expression pattern similar to that of *S.*
537 *japonicum* schistosomula, whereas on the surface of *S. bovis* adults the annexin is

538 expressed less abundantly than in *S. japonicum* adult worms (Tararam et al., 2010).
539 Additionally, the SbANX described in this work is homologous to Smp_074150. This *S.*
540 *mansoni* annexin was detected by mass spectrometry of material released by trypsin
541 shaving of live *S. mansoni* (Castro-Borges et al., 2011), providing additional support to
542 the notion that SbANX, as Smp_074150, might also be surface-located.

543 Bearing in mind these results, it is somewhat surprising that annexin, despite
544 being expressed on the surface of the tegument and also found in the secretion-excretion
545 products, should not be immunogenic in natural infections by *Schistosoma* (Mutapi et
546 al., 2005; Pérez-Sánchez et al., 2006). It would be interesting to test if vaccination with
547 this protein will lead to its recognition by the host immune system allowing the
548 evaluation of its protective potential against infections in ruminant schistosomiasis.

549 In sum, here we have cloned, sequenced and characterized a *S. bovis* annexin.
550 We show that, *in vitro*, the corresponding recombinant protein displays fibrinolytic and
551 anticoagulant activities; that the native protein is expressed on the tegument surface of
552 adult worms and schistosomula, and that it is therefore in direct contact with the host's
553 blood. All this suggests that this annexin could be used by *S. bovis*, together with other
554 tegument proteins of proven fibrinolytic activity, such as enolase, to prevent thrombus
555 formation and other haemostatic disturbances that could be lethal for the survival of the
556 parasite in the bloodstream. The anti-haemostatic activities observed, and other potential
557 immune modulatory functions make the *S. bovis* annexin and its homologues promising
558 antigenic targets for development of new anti-schistosome vaccines.

559

560 **Acknowledgements**

561 This research was funded by project AGL2007-60413/GAN, granted by the
562 Spanish Ministry of Science and Innovation. E. De la Torre-Escudero is holder of a
563 Ministry of Science and Innovation predoctoral grant and R. Manzano-Román is funded
564 by the JAEDoc program (CSIC-FSE).

565

566

567

568 **References**

569 Abath, F.G., Werkhauser, R.C., 1996. The tegument of *Schistosoma mansoni*:
570 functional and immunological features. *Parasite Immunol.* 18, 15-20.

571 Agnew, A.M., Murare, H.M., Lucas, S.B., Doenhoff, M.J., 1989. *Schistosoma bovis* as
572 an immunological analogue of *S. haematobium*. *Parasite Immunol.* 11, 329-340.

573 Arnold, K., Bordoli, L., Kopp, J., and Schwede, T., 2006. The SWISS-MODEL
574 Workspace: A web-based environment for protein structure homology modelling.
575 *Bioinformatics*, 22,195-201.

576 Bendtsen, J.D., Nielsen, H., von Heijne, G., Brunak, S., 2004. Improved prediction of
577 signal peptides: SignalP 3.0. *J. Mol. Biol.* 340, 783-795.

578 Braschi, S., Curwen, R.S., Ashton, P.D., Verjovski-Almeida, S., Wilson, A., 2006. The
579 tegument surface membranes of the human blood parasite *Schistosoma mansoni*: a
580 proteomic analysis after differential extraction. *Proteomics* 6, 1471-1482.

581 Braschi, S., Wilson, R.A., 2006. Proteins exposed at the adult schistosome surface
582 revealed by biotinylation. *Mol. Cell. Proteomics* 5, 347-356.

583 Castro-Borges, W., Dowle, A., Curwen, R.S., Thomas-Oates, J., Wilson, R.A., 2011.
584 Enzymatic shaving of the tegument surface of live schistosomes for proteomic

585 analysis: a rational approach to select vaccine candidates. PLoS. Negl. Trop. Dis. 5,
586 e993.

587 Cederholm, A., Frostegård, J., 2007. Annexin A5 as a novel player in prevention of
588 atherothrombosis in SLE and in the general population. Ann. N. Y. Acad. Sci. 1108,
589 96-103.

590 De la Torre-Escudero, E., Manzano-Román, R., Pérez-Sánchez, R., Siles-Lucas, M.,
591 Oleaga, A., 2010. Cloning and characterization of a plasminogen-binding surface-
592 associated enolase from *Schistosoma bovis*. Vet. Parasitol. 173, 76-84.

593 DeLano, W.L., 2002. The PyMOL Molecular Graphics System. DeLano Scientific, Palo
594 Alto, CA, USA.

595 Draeger, A., Monastyrskaya, K., Babiychuk, E.B., 2011. Plasma membrane repair and
596 cellular damage control: The annexin survival kit. Biochem. Pharmacol. 15, 703-
597 712.

598 Eisenhaber, B., Bork, P., Yuan, Y., Loeffler, G., Eisenhaber, F., 2000. Automated
599 annotation of GPI anchor sites: case study *C.elegans*. TIBS 25, 340-341.

600 Gao, Y.J., Yan, H.L., Ding, F.X., Lu, Y.M., Sun, S.H., 2007. Annexin B1 at the host-
601 parasite interface of the *Taenia solium* cysticercus: Secreted and associated with
602 inflammatory reaction. Acta Trop. 101,192-199.

603 Gerke, V., Moss, S.E., 2002. Annexins: from structure to function. Physiol. Rev. 82,
604 331-371.

605 Gui, M., Kusel, J.R., Shi, Y.E., Ruppel, A., 1995. *Schistosoma japonicum* and *S.*
606 *mansoni*: comparison of larval migration patterns in mice. J. Helminthol. 69, 19-25.

607 Hajjar, K.A., Krishnan, S., 1999. Annexin II: A mediator of the plasmin/plasminogen
608 activator system. Trends Cardiovasc. Med. 9,128-138.

609 Hajjar, K.A., Mauri, L., Jacovina, A.T., Zhong, F., Mirza, U.A., Padovan, J.C., Chait,
610 B.T., 1998. Tissue plasminogen activator binding to the annexin II tail domain.
611 Direct modulation by homocysteine. *J. Biol. Chem.* 273, 9987-9993.

612 Hofmann, A., Osman, A., Leow, C.Y., Driguez, P., McManus, D.P., Jones, M.K., 2010.
613 Parasite annexins-new molecules with potential for drug and vaccine development.
614 *Bioessays* 32, 967-976.

615 Jones, M.K., Gobert, G.N., Zhang, L., Sunderland, P., McManus, D.P., 2004. The
616 cytoskeleton and motor proteins of human schistosomes and their roles in surface
617 maintenance and host-parasite interactions. *Bioessays* 26, 752-765.

618 Moss, S.E., Morgan, R.O., 2004. The annexins. *Genome Biol.* 5, 219.

619 Mountford, A.P., 2005. Immunological aspects of schistosomiasis. *Parasite Immunol.*
620 27, 243-246.

621 Mulvenna, J., Moertel, L., Jones, M.K., Nawaratna, S., Lovas, E.M., Gobert, G.N.,
622 Colgrave, M., Jones, A., Loukas, A., McManus, D.P., 2010a. Exposed proteins of
623 the *Schistosoma japonicum* tegument. *Int. J. Parasitol.* 40, 543-554.

624 Mulvenna, J., Sripa, B., Brindley, P.J., Gorman, J., Jones, M.K., Colgrave, M.L., Jones,
625 A., Nawaratna, S., Laha, T., Suttiaprapa, S., Smout, M.J., Loukas, A., 2010b. The
626 secreted and surface proteomes of the adult stage of the carcinogenic human liver
627 fluke *Opisthorchis viverrini*. *Proteomics* 10, 1063-1078.

628 Mundodi, V., Kucknoor, A.S., Alderete, J.F., 2008. Immunogenic and plasminogen-
629 binding surface-associated alpha-enolase of *Trichomonas vaginalis*. *Infect. Immun.*
630 76, 523-531.

631 Mutapi, F., Burchmore, R., Mduluzza, T., Foucher, A., Harcus, Y., Nicoll, G., Midzi, N.,
632 Turner, C.M., Maizels, R.M., 2005. Praziquantel treatment of individuals exposed to

633 *Schistosoma haematobium* enhances serological recognition of defined parasite
634 antigens. J. Infect. Dis. 192, 1108-1118.

635 Oleaga-Pérez, A., Pérez-Sánchez, R., Astigarraga, A., Encinas-Grandes, A., 1994.
636 Detection of pig farms with *Ornithodoros erraticus* by pig serology. Elimination of
637 non-specific reactions by carbohydrate epitopes of salivary antigens. Vet. Parasitol.
638 52, 97-111.

639 Pearce, E.J., MacDonald, A.S., 2002. The immunobiology of schistosomiasis. Nature
640 Rev. Immunol. 2, 499-511.

641 Pérez-Sánchez, R., Ramajo-Hernández, A., Ramajo-Martín, V., Oleaga, A., 2006.
642 Proteomic analysis of the tegument and excretory-secretory products of adult
643 *Schistosoma bovis* worms. Proteomics 6, 226-236.

644 Pérez-Sánchez, R., Valero, M.L., Ramajo-Hernández, A., Siles-Lucas, M., Ramajo-
645 Martín, V., Oleaga, A., 2008. A proteomic approach to the identification of
646 tegumental proteins of male and female *Schistosoma bovis* worms. Mol. Biochem.
647 Parasitol. 161, 112-23.

648 Ramajo-Hernández, A., Pérez-Sánchez, R., Ramajo-Martín, V., Oleaga, A., 2007.
649 *Schistosoma bovis*: plasminogen binding in adults and the identification of
650 plasminogen-binding proteins from the worm tegument. Exp. Parasitol. 115, 83-91.

651 Secor, W.E., 2005. Immunology of human schistosomiasis: off the beaten path. Parasite
652 Immunol. 27, 309-316.

653 Skelly, P.J., Wilson, R.A., 2006. Making sense of the schistosome surface. Adv.
654 Parasitol. 63:185-284.

655 Tararam, C.A., Farias, L.P., Wilson, R.A., Leite, L.C., 2010. *Schistosoma mansoni*
656 Annexin 2: molecular characterization and immunolocalization. Exp. Parasitol, 126,
657 146-155.

658 van Balkom, B.W., van Gestel, R.A., Brouwers, J.F., Krijgsveld, J., Tielens, A.G.,
659 Heck, A.J., van Hellemond, J.J., 2005. Mass spectrometric analysis of the
660 *Schistosoma mansoni* tegumental sub-proteome. J. Proteome Res. 4, 958-966.

661 van Hellemond, J.J., Retra, K., Brouwers, J.F., van Balkom, B.W., Yazdanbakhsh, M.,
662 Shoemaker, C.B., Tielens, A.G., 2006. Functions of the tegument of schistosomes:
663 clues from the proteome and lipidome. Int. J. Parasitol. 36, 691-699.

664 Vercruysse, J., Gabriel, S., 2005. Immunity to schistosomiasis in animals: an update.
665 Parasite Immunol. 27, 289-295.

666 Wang, K., Guo, Y., Li, K., Lu, Y., Zhang, Y., Sun, S., Yan, H., Zhang, S., 2006.
667 Molecular characterization and anticoagulant activity of a novel annexin derived
668 from the *Taenia solium*. Acta Trop. 99, 165-172.

669 Winter, A., Yusof, A.M., Gao, E., Yan, H.L., Sun, S.H., Hofmann, A., 2006.
670 Biochemical characterization of annexin B1 from *Cysticercus cellulosae*. FEBS J,
671 273, 3238-3247.

672 Yan, H.L., Xue, G., Mei, Q., Ding, F.X., Wang, Y.Z., Sun, S.H., 2008. Calcium-
673 dependent proapoptotic effect of *Taenia solium* metacestodes annexin B1 on human
674 eosinophils: a novel strategy to prevent host immune response. Int. J. Biochem. Cell.
675 Biol. 40, 2151-2163.

676

677

678 **Figure legends.**

679

680 Figure 1. (A) Alignment of the SbANX (ACC78610) with annexins B1 (AAD34598)
681 and B2 (AAY17503) from *Taenia solium* and human A2 (AAH09564) and A5
682 (NP_001145). The conserved amino acids are labelled with asterisks; the conservative
683 and semi-conservative substitutions are labelled with two and one points, respectively.
684 Predicted α -helices are indicated in grey and β -sheets in green. The four-repeat domains
685 of the annexin sequence are indicated with a horizontal line over the conserved zone.
686 The type II Ca^{2+} - binding sites are shaded in yellow, and the type III Ca^{2+} - binding sites
687 are underlined. The t-PA-binding motif of human A2 annexin and other similar motifs
688 identified in the SbANX and in the *T. solium* B2 annexin are in red. The phospholipid-
689 binding motif of the cell surface identified in the human A2 annexin is boxed in. (B),
690 Molecular modelling of *S. bovis* annexin and human A2 annexin. The variable N-
691 terminal end is in black; and the annexin repeat domains I, II, III and IV are in red,
692 yellow, orange and blue respectively. The insert fragment in the linker region between
693 repeats II and III is in green.

694

695 Figure 2. (A) Plasminogen-binding assay to 0.5 μg of rSbANX and incubation with
696 increasing amounts of plasminogen, 0-3 μg (\blacklozenge). Positive control using 1 μg of tegument
697 extract (TG) instead of rSbANX (\mathbf{X}). Negative control coated with BSA (\blacksquare). (B)
698 Competition assay. Wells coated with 0.5 μg of rSbANX (\blacklozenge) or BSA (\blacksquare) were
699 incubated with 0.5 μg of plasminogen and increasing amounts of ϵACA . Each point is
700 the mean of three replicates \pm standard deviation.

701

702 Figure 3. Plasminogen activation assay with rSbANX or t-PA alone, rSbANX together
703 with t-PA, and the negative control with the reaction substrate alone. Each point is the
704 mean of four replicates \pm standard deviation. The experiments were performed three
705 times.

706 Figure 4. Coagulation assays in plasma samples with increasing concentrations of
707 rSbANX (0-80 μ g/ml). (A) Prothrombin time assay (PT) expressed in time and
708 percentage of activity. (B) Activated partial thromboplastin time (aPTT). (■) rSbANX,
709 (□)BSA and (□) buffer. Each point is the mean of two replicates \pm standard deviation.
710 The experiments were performed two times. * $p < 0.001$.

711

712 Figure 5. Western blot for study of the specificity of an anti-rSbANX serum on the
713 rSbANX and a tegument extract (TG) from *S. bovis* adult worms. 1, negative control
714 sera; 2, anti-rSbANX rabbit serum at 1:1,600 dilution.

715

716 Figure 6. Immunolocalization of *S. bovis* annexin in lung-schistosomula. Confocal
717 microscope images of schistosomula after incubation with phalloidin-Alexa Fluor 488
718 (green) plus the negative or the anti-rSbANX rabbit sera and an anti rabbit IgG-Alexa
719 Fluor 594 (red). Magnification 600x.

720

721 Figure 7. Immunolocalization of *S. bovis* annexin in adult worms. (A) Images of
722 parasite sections, (B) magnification of the boxes highlighted in (A) showing the male
723 and female tegument, and (C) images of whole parasites. Both, the sections and whole
724 parasites were incubated with phalloidin-Alexa Fluor 488 (green) plus the negative or

725 the anti-rSbANX rabbit sera and an anti-rabbit IgG-Alexa Fluor 594 (red). The upper
726 row of panels (A) and (C) shows the merged projected images derived from sections
727 generated by the confocal microscope and the lower row shows the corresponding
728 transmitted light images. Magnification 600x.

729

730

731

732

Figure 1
[Click here to download high resolution image](#)

Figure 1

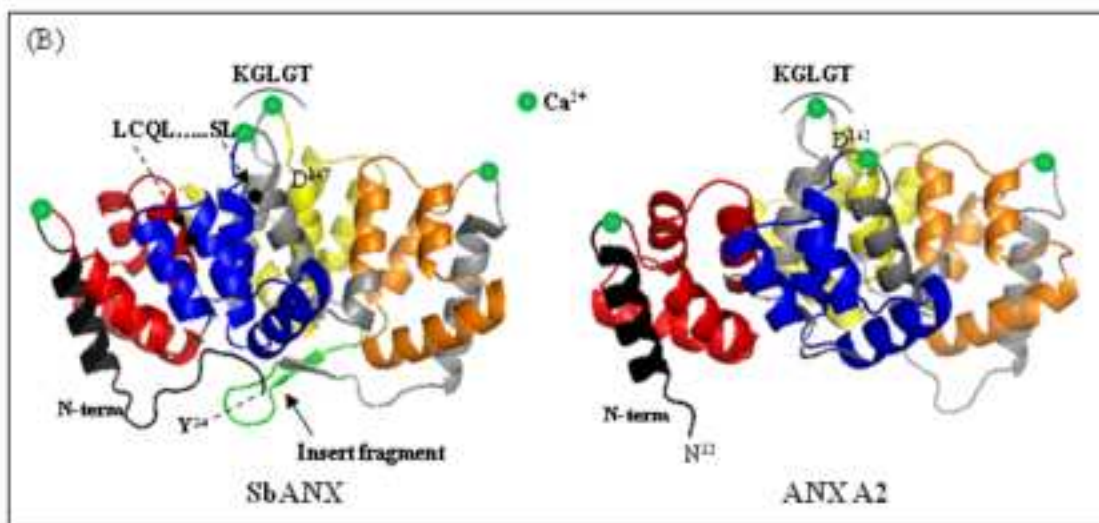
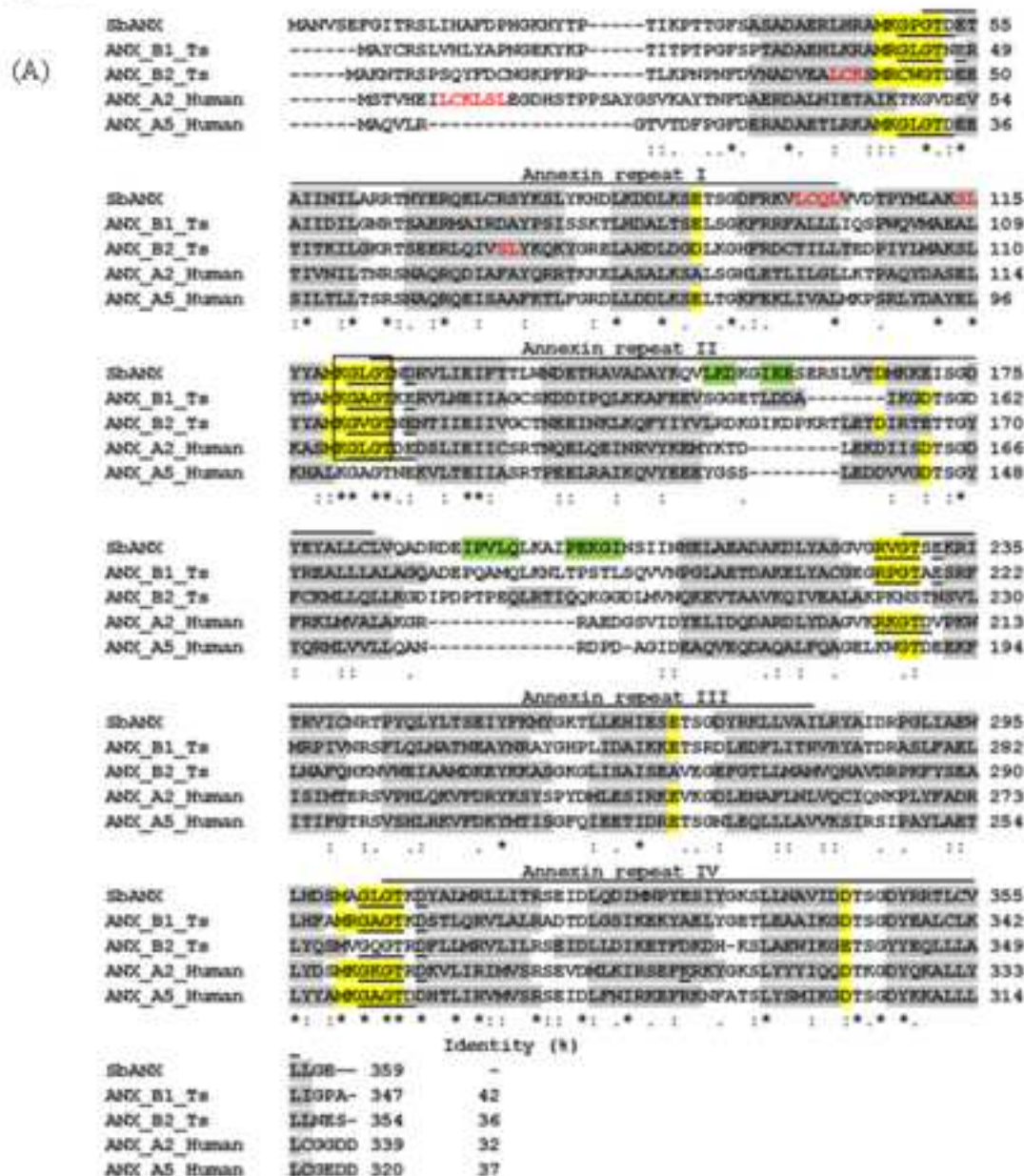


Figure 2

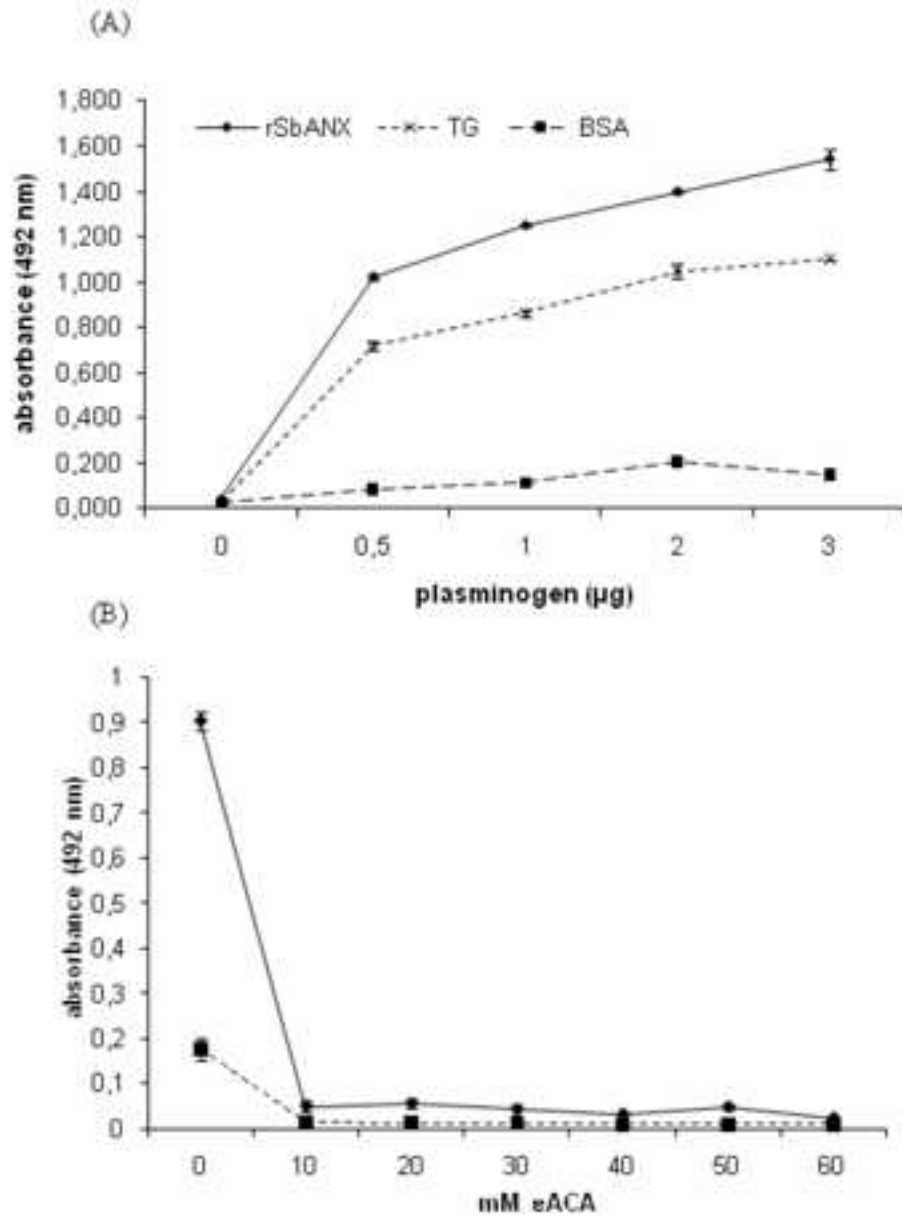


Figure 3

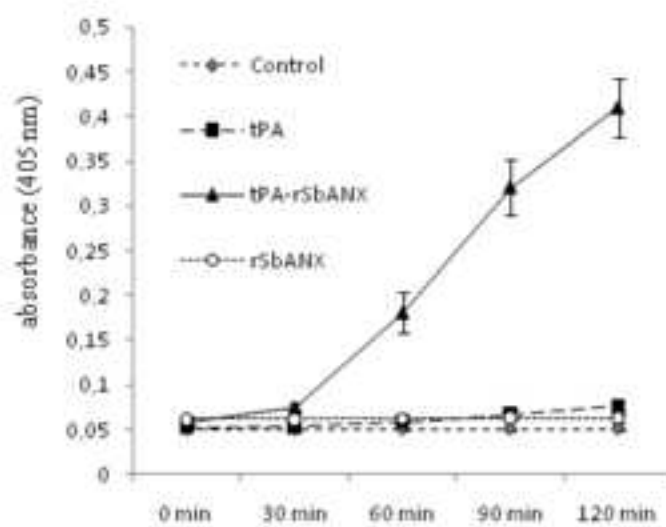


Figure 4

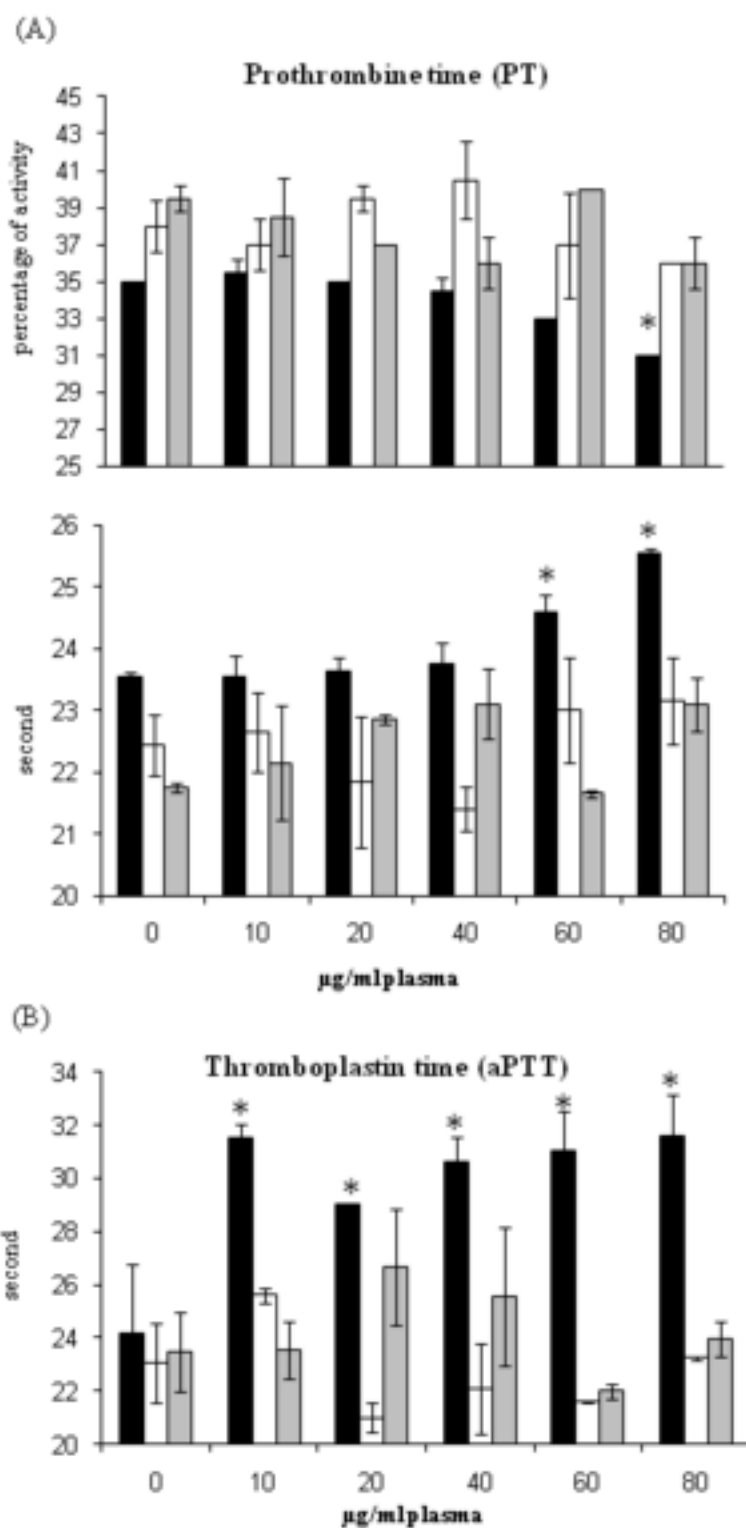


Figure 5

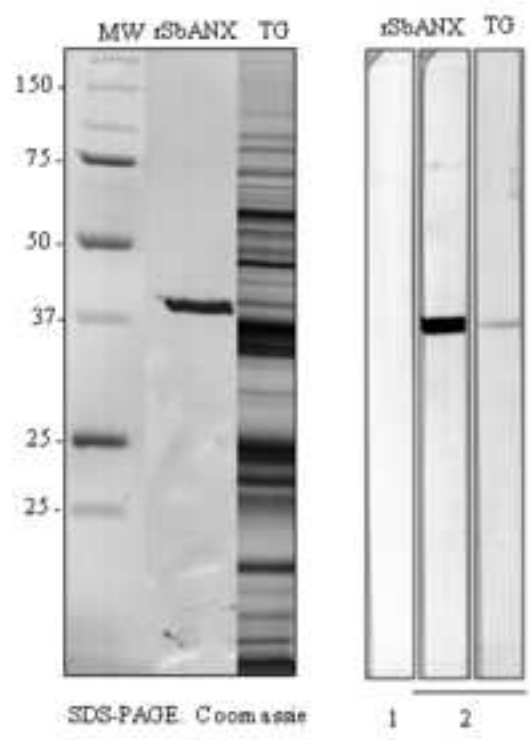


Figure 6

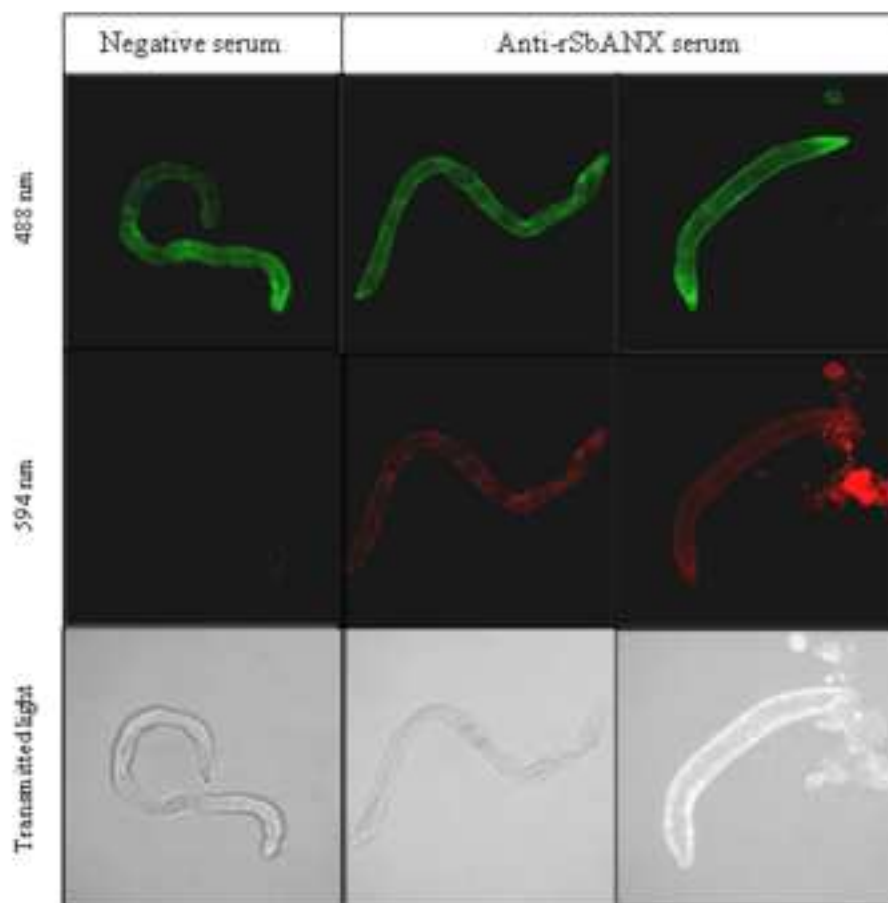


Figure 7

